ELSEVIER

Journal of Chromatography A, 965 (2002) 35–49

JOURNAL OF CHROMATOGRAPHY A

www.elsevier.com/locate/chroma

Review

Monolithic silica columns for high-efficiency chromatographic separations

Nobuo Tanaka[a,*], Hiroshi Kobayashi[a], Norio Ishizuka[b], Hiroyoshi Minakuchi[b], Kazuki Nakanishi[b], Ken Hosoya[a], Tohru Ikegami[a]

[a]*Department of Polymer Science and Engineering, Kyoto Institute of Technology, Matsugasaki, Sakyo-ku, Kyoto 606-8585, Japan*

[b]*Department of Material Chemistry, Graduate School of Engineering, Kyoto University, Yoshida, Sakyo-ku, Kyoto 606-8501, Japan*

Abstract

Studies on the structural and chromatographic properties of monolithic silica columns were reviewed. Monolithic silica columns prepared from tetraalkoxysilane by a sol–gel method showed high efficiency and high permeability on the basis of the small-sized silica skeletons, large-sized through-pores, and resulting through-pore size/skeleton size ratios much larger than those found in a particle-packed column.

Keywords: Reviews; Monolithic silica columns; Stationary phases, LC; Columns

Contents

1. Introduction

Chromatographers have been obtaining higher efficiency in a shorter period of time by reducing the size of HPLC packing materials for decades. The number of theoretical plates obtainable by using a single column, however, has been relatively steady at 10 000–25 000 in HPLC. This is due to the high pressure drop associated with small-sized packing materials under the limitation of operating pressure at 350–400 kg/cm^2 with current instrumentation. A compromise has been necessary between column efficiency desired and the pressure drop of the column by adjusting the column length. Higher

*Corresponding author. Tel.: +81-75-724-7809; fax: +81-75-724-7710.

E-mail address: nobuo@ipc.kit.ac.jp (N. Tanaka).

0021-9673/02/$ – see front matter
PII: S0021-9673(01)01582-5

performance beyond the limit has been achieved recently in ultrahigh pressure liquid chromatography (UHPLC) by utilizing higher operational pressure, in capillary electrochromatography (CEC) by utilizing electroosmotic flow, or by employing a monolithic column having a network structure instead of a particle-packed column in HPLC.

The limit in performance of HPLC columns (and the reasons for the compromise) can be described as follows. Eqs. (1)–(9) define or express the properties of packing materials and columns [1–3] including the efficiency and flow resistance, where N stands for the number of theoretical plates, L the column length, H a height equivalent of a theoretical plate, σ^2 dispersion of a solute band, d_p particle size, u linear velocity of mobile phase, D_m diffusion coefficient of a solute in the mobile phase, C_x coefficient for the contribution of each term, h reduced plate height, ν reduced velocity, ϕ flow resistance parameter, ΔP column pressure drop, t_0 column dead time, η solvent viscosity, K column permeability, and E separation impedance:

$$H = \sigma^2/L = L/N \tag{1}$$

$$\begin{aligned} H &= 1/[(1/C_e d_p) + (D_m/C_m d_p^2 u)] + C_d D_m/u \\ &\quad + C_{sm} d_p^2 u/D_m \\ &= Au^{1/3} + B/u + Cu \end{aligned} \tag{2}$$

$$h = A\nu^{1/3} + B/\nu + C\nu \tag{3}$$

$$h = H/d_p \tag{4}$$

$$\nu = ud_p/D_m = (u/d_p)/(D_m/d_p^2) \tag{5}$$

$$\phi = \Delta P t_0 d_p^2/\eta L^2 \tag{6}$$

$$K = u\eta L/\Delta P, u = L/t_0 \tag{7}$$

$$E = \Delta P t_0/\eta N^2 = (\Delta P/N)(t_0/N)(1/\eta) \tag{8}$$

$$t_0 = h^2 \phi N^2 \eta/\Delta P \tag{9}$$

The reduction of particle size can lead to better column efficiency on the basis of the smaller contribution of eddy diffusion and mobile-phase mass transfer (A-term) and the shorter diffusion path length (C-term) as indicated by Eq. (2). The plots of plate time against the number of theoretical plates shown in Fig. 1 indicate that the reduction in particle size actually contributes to the reduction in separation time with smaller maximum plate numbers attainable under a given time and pressure drop [2]. The curves in Fig. 1 were obtained for a particle size of 1–10 μm and an operating pressure of 400 kg/cm^2 that is the limit of most commercial equipment. The envelope for the curves obtained for various d_p values represents the limit of performance of a particle-packed column in HPLC obtainable under a practical pressure limit of a conventional pump. Under optimized HPLC conditions, a conventional particle-packed column would produce 100 000 theoretical plates with $t_0 = 1000$ s at pressure drop of 400 kg/cm^2 by using 4-μm particles. If comparison is made at constant efficiency (N), one can readily realize the reduction in t_0 with smaller d_p, while the pressure drop (ΔP) is inversely proportional to d_p^2 (Eq. (6)). This is why small particles in a range of 1.5–3 μm have been used in a short column for fast separations. There is a limit in total performance

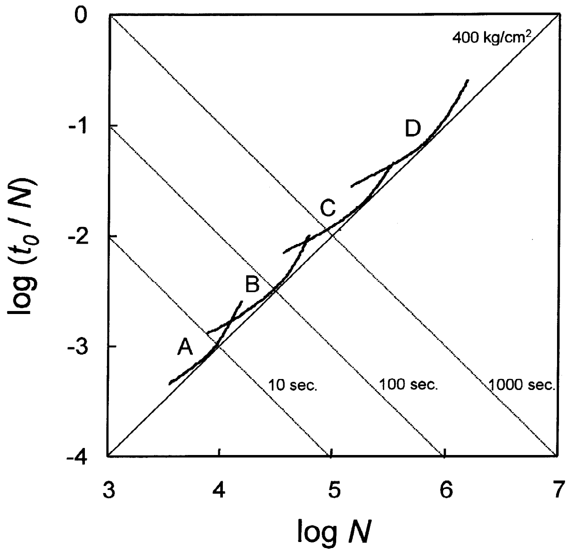

Fig. 1. Plots of plate time, (t_0/N), vs. plate number for a particle-packed column in HPLC (adopted from Ref. [2]). The curves were obtained by assuming the parameters, maximum pressure: 400 kg/cm^2, $\eta = 0.001$ Pa/s, $\phi = 1000$, $D_m = 1\times10^{-9}$ m^2/s, and Knox equation $h = \nu^{1/3} + 1.5/\nu + 0.05\nu$. Particle diameter: (A) 1 μm, (B) 2 μm, (C) 5 μm, (D) 10 μm. The dotted lines indicate the required t_0 values in seconds.

($N^2/t_0\ \Delta P$, cf. Eq. (8)) of a column packed with particles of certain size. The concept is known as the Knox–Saleem optimum described by the basic chromatographic parameters, t_0, N, and ΔP in Eq. (9) [2], and represented by the envelope for the group of curves for various particle sizes in Fig. 1.

The most straightforward approach to a higher N and a shorter separation time in HPLC is to use a higher pressure, as realized in UHPLC [4,5]. Another way to generate a large N by using small particles in a long column is to utilize an electroosmotic flow (EOF) in CEC [6]. The problem of high-pressure drop can also be alleviated by using an open-tube column [2] or the operation of a column at high temperatures [7] that can increase N or shorten t_0 by increasing permeability or by facilitating solute diffusion. All these approaches can overcome the high-pressure drop associated with a column having a tightly packed bed creating small interstitial openings with a (through-pore (interstitial void) size)/(particle size) ratio of 0.25–0.4 [8]. Effort is being made in these approaches to solve the problems in instrumentation or in execution.

An increase in column performance can also be obtained by increasing the column permeability (K, Eq. (7)). One possible way to attain higher permeability is to use a monolithic column, which is defined as a column consisting of one piece of solid that possesses interconnected skeletons and interconnected flow paths (through-pores) through the skeletons. A monolithic column with small-sized skeletons and large through-pores can simultaneously reduce the diffusion path length and flow resistance compared to a particle-packed column. Thus a support structure having a large (through-pore size)/(skeleton size) ratio, that is not possible with a particle-packed column, can provide both high permeability and high column efficiency in HPLC. A wide range of monoliths, either capillary-sized or larger-sized, have been reported.

It has been attempted to use continuous porous polymer beds as separation media [9–18]. Monolithic polymer columns made of organic materials enabled high-speed separation of polypeptides and proteins in reversed-phase and in ion-exchange chromatography, but showed relatively low efficiency for small solutes. It has also been reported that monolithic columns can be prepared by sintering or by embedding silica particles, after packing the particles into a capillary [19–23]. In principle, however, such columns prepared by the modification of a packed bed will not be able to escape from the limitations associated with particle-packed columns. In CEC, slightly lower performance was reported for these columns compared to particle-packed columns.

Recently, Nakanishi et al. reported the preparation of silica gel monoliths with a broad range of through-pores as well as with mesopores of a 10 nm range [24,25]. The process resulting in the silica monoliths with double pore structures by a sol–gel method starting from alkoxysilanes in the presence of water-soluble organic polymers has been summarized recently [26]. Minakuchi et al. and others reported that continuous porous silica columns allowing high (through-pore size)/(skeleton size) ratios based on the controllable sizes of silica skeletons, through-pores, and mesopores provided higher column efficiency and lower pressure drop than conventional columns packed with particles [27–37]. Here we will review the results of our study on the properties of monolithic silica columns prepared by a sol–gel method.

2. Preparation method of monolithic silica columns

Monolithic silica columns can be prepared either in a mold (a 6–9 mm I.D. glass test tube) or in a fused-silica capillary, as described previously [26,28,33]. Silanes such as tetramethoxysilane (TMOS) or tetraethoxysilane undergo hydrolytic polymerization in aqueous acetic acid in the presence of polyethylene glycol (PEG) to form monolithic silica having network structures. The preparation in a mold is accompanied by the volume reduction of the whole structure. The diameters of products are ca. 4.6 or 7 mm when one uses a mold of 6 and 9 mm I.D., respectively. The resulting silica monoliths were covered with PTFE tubing or with PEEK resin to fabricate a column for HPLC. Long columns cannot be prepared to be straight, limiting the column length to about 15 cm or shorter. The PTFE-covered monolith (MS-PTFE) was used in an external pressurizing device, a Z-module (Waters). The PEEK-covered columns (MS-PEEK) can withstand inlet pressure of up to 120 kg/cm^2. This type of monolithic silica columns, Chromolith, is commercially available at 5- or 10-cm length.

The silica network structure must be attached to the tube wall to prepare a monolith in a fused-silica capillary (MS-FS) in order to prevent shrinkage of the skeletons. Smaller diameter tubes (50 μm I.D.) gave better results than larger-sized tubes. After the formation of the network structure of silica skeletons, mesopores were formed by the treatment with ammonia introduced after the formation of silica skeletons. Nakanishi et al. reported the preparation method of mesopores that can be tailored by aging in ammonia solution formed by the hydrolysis of urea [25]. The addition of urea in the starting preparation mixture has made the process simpler, since the mesopores can be prepared just by heating the whole reaction mixture in the capillary. The monolithic silica column in a capillary can be used after on-column chemical modification with *N*,*N*-diethylaminodimethyloctadecylsilane. The columns were used without retaining frits.

3. Structural properties of monolithic silica columns

The macroporous structure of monolithic silica was prepared via spinodal decomposition by which the periodic domains (silica-rich and solvent-rich domains) were developed from the initial homogeneous solution. The network structure is then frozen by gelation caused by the progress of polymerization. By controlling the composition of the starting mixture, or the concentration of TMOS and PEG, one can control the size of silica skeletons and through-pores independently. Thus it is possible to produce monolithic silica columns having through-pore size/skeleton size ratios much greater than those found in a particle-packed column.

SEM photographs of the monolithic silica columns in Fig. 2 show that both the silica skeletons and the through-pores are co-continuous and the domain size (a combined size of through-pore and skeleton) decreases with the increase in PEG content in the starting mixture. The domain size frozen in the gel depends on how far the coarsening of the domains can proceed until they are frozen-in by the sol–gel transition [24]. In the present case, the increase in the concentration of PEG in the starting composition leads to retarded onset of phase separation relative to the sol–gel transition, and the smaller domain size. As a result of the later phase separation, the phase domains are frozen in the earlier stage of the coarsening, and finer domains are observed in gelled samples.

Fig. 2e–h shows the SEM photographs of the fractured surfaces of the monolithic silica columns prepared in a capillary. The shrinkage of silica skeletons formed large voids along the wall of a 250-μm-diameter capillary (Fig. 2e). The attachment of the silica skeletons to the tube wall of a small-diameter capillary that has the greater wall area/volume ratio prevented the shrinkage of the whole network structure, while resulting in large interstitial voids (through-pores). The clusters of uniform-sized silica skeletons of about 2 μm and through-pores of various sizes of up to 10 μm were distributed in the 50 μm I.D. capillary (Fig. 2f–h). The morphologies of silica prepared in a capillary possess the appearance of aggregates of silica spheres, or a corpuscular system [38], that is different from the network structures of relatively smooth cylindrical skeletons, or a spongy system, found with large-sized skeletons of monolithic silica columns prepared in a mold shown in Fig. 2a and b. The present silica skeleton structures in a capillary indicates that the phase separation relative to the gelation proceeded further as compared with the case of the silica monoliths prepared in a mold.

Since the micrometre-range structures were formed by spinodal decomposition, the structures of skeletons and voids were expected to have self similarity [39]. Therefore, when the concentration ratio of TMOS to acetic acid in aqueous solution was kept constant with a minor change in PEG content, the ratio of the silica skeleton size to the through-pore size was nearly constant and all the monolithic silica gels were expected to have similar through-pore volume. Fig. 3a shows the through-pore size distribution measured by mercury porosimetry. The sharp distributions of the pore sizes around 1.3, 1.7, 2.3 and 3.4 μm were found corresponding to the amounts of PEG 10.4, 10.2, 9.8 and 9.4 g per 100 ml aqueous acetic acid in the starting mixture, respec-

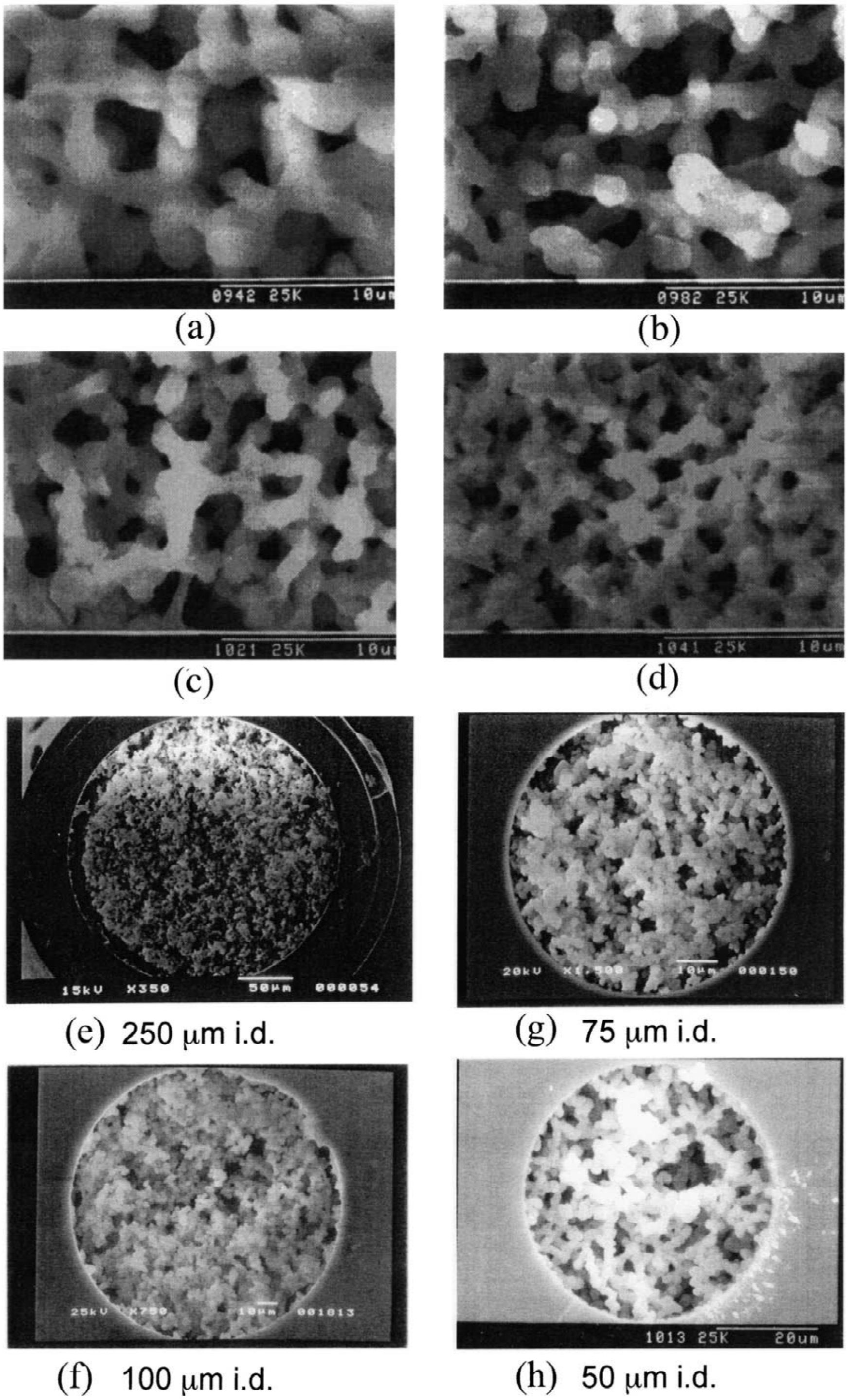

Fig. 2. (a–d) SEM photographs of monolithic silica MS-PTFE(A)–(D) prepared from the compositions A–D in Table 1 [29]. The bars denote 10 μm in all photographs. (e–h) Scanning electron micrographs of monolithic silica prepared in fused-silica capillaries prepared in (e) 250 μm, (f) 100 μm, (g) 75 μm, and (h) 50 μm (MS-FS(50)) diameter [37].

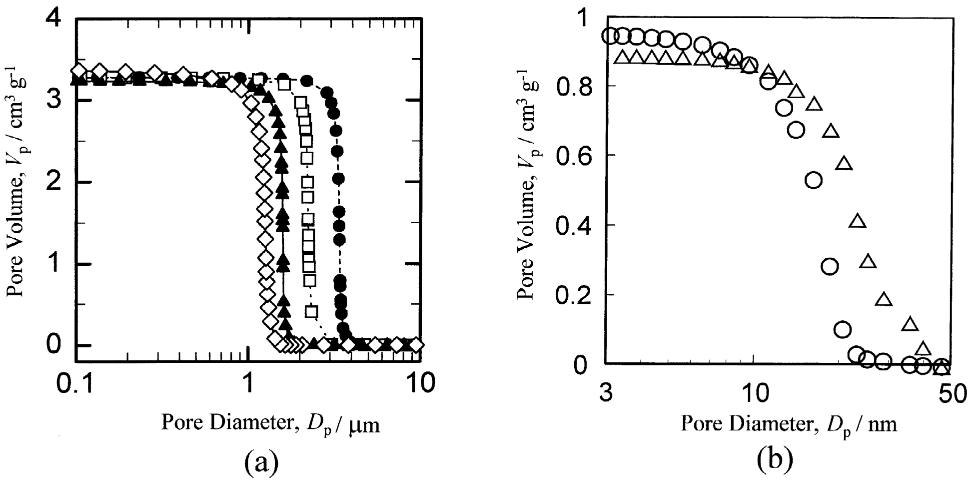

Fig. 3. (a) Pore-size distribution curves of gel samples identical to those shown in Fig. 2a–d by mercury porosimetry [29]. A (●), B (□), C (▲), D (◇). (b) Pore-size distribution curves of mesopores in the silica skeletons measured by nitrogen adsorption. MS-PTFE(A)-S (○), MS-PTFE(A)-L (△).

tively, as shown in Table 1. The pore volumes were found to be constant at ca. 3.2 cm^3/g, as expected.

The size of through-pores of monolithic silica in capillary was much larger than the skeleton size resulting in the through-pore size/skeleton size ratio of up to 3–5. Through-pore size/skeleton size ratios were reported to be 0.25–0.4 with a column packed with particles [8], and found to be 1.2–1.5 for monolithic silica columns prepared in a mold with shrinkage of the whole network structures [29].

The mesopores of 10–25 nm size were formed by changing pH and temperature of the reaction mixture following silica preparation [24,25]. Fig. 3b shows the size distributions of the mesopores measured by

Table 1
Composition of the preparation mixtures and the concentration of ammonium hydroxide, and the pore properties of the produced silica gels [29]

Silica rod no.	Amount of PEG[a] (g)	NH_4OH[b] (mol/l)	Mesopore size[c] (nm)	Domain size[d] (μm)	Through pore size[e] (μm)
MS-PTFE(A)-L	9.4	1.0	25.2	5.88	3.46
MS-PTFE(A)-S	9.4	0.01	15.7	5.70	3.39
MS-PTFE(B)-L	9.8	1.0	25.2	3.85	2.18
MS-PTFE(B)-S	9.8	0.01	15.8	3.81	2.23
MS-PTFE(C)-L	10.2	1.0	23.2	2.97	1.68
MS-PTFE(C)-S	10.2	0.01	13.1	2.89	1.73
MS-PTFE(D)-L	10.4	1.0	23.6	2.27	1.28
MS-PTFE(D)-S	10.4	0.01	15.5	2.32	1.26

[a] PEG added to 4 ml of TMOS and 100 ml of 0.01 *M* aqueous acetic acid.
[b] Concentration of NH_4OH used for controlling mesopore size after the preparation of a silica gel.
[c] Measured by nitrogen adsorption.
[d] Measured from SEM photographs.
[e] Measured by mercury porosimetry.

nitrogen adsorption method. The gels treated with a 0.01 or 1.0 *M* aqueous ammonium hydroxide solution possess the pores distributed around 16 nm and 24 nm with surface areas of 340 and 140 m^2/g and pore volumes of 0.96 and 0.90 cm^3/g, respectively. These values were similar to those of the silica gel particles used for HPLC [8].

The porosity of monolithic silica columns is much greater than that of a column packed with particles, as shown in Table 2. Major difference was seen in the external porosities, 39% for a particle-packed column, 65–70% for MS-PTFE and MS-PEEK prepared in a mold, and higher than 80% for MS-FS prepared in a capillary, as determined by size exclusion chromatography (SEC). With the small amount of silica skeleton in MS-FS, total porosity exceeds 90% of the column volume and less than 10% occupied by the silica skeletons. The porosity of silica skeletons was similar to that of monolithic silica columns prepared in a mold. The phase ratio decreased accordingly to less than 0.02–0.05 for MS-FS, compared to ca. 0.06 for MS-PTFE, and 0.19 for a column packed with the C_{18}-silica particles, as estimated by the porosity measurement before and after the bonding reaction as well as the comparison of retention factors (*k* values) [33]. The monolithic silica columns in the capillary, however, possess greater phase ratios than an open tube column or a column packed with 2-μm nonporous particles, leading to higher sample loading capacity.

4. Chromatographic properties

Major chromatographic features of monolithic silica columns arise from the large through-pore size/skeleton size ratios and high porosities, resulting in high permeability and large number of theoretical plates per unit pressure drop.

Fig. 4 compares the pressure drop of columns in 80% methanol. The pressure drop of the MS-PTFE monolith (through-pore size = 2.2 μm, skeleton size = 1.6 μm) was about 1/4 that of Mightysil (a column packed with 5-μm ODS particles). The pressure drop of MS-FS(50) (through-pore size = 8 μm, skeleton size = 2 μm) was even lower than that of the MS-PTFE columns. The smaller flow resistance of the former monolith is due to the presence of much larger through-pores in the order of 8–10 μm. Such large flow paths would be found in a column packed with 30–40-μm particles. MS-PEEK monolith showed lower pressure drop compared to the columns packed with 5-μm particles, but higher compared with MS-PTFE. Typical *K* values, reflecting the column permeability, are 4×10^{-13}, 1×10^{-12}, 7×10^{-14}, and 4×10^{-14} m^{-2} for MS-PTFE, MS-FS, MS-PEEK, and a column packed with 5-μm particles, respectively. The results indicate that monolithic silica columns having large-sized through-pores and high porosity resulted in high permeability.

High permeability and small diffusion path length

Table 2
Porosity of columns [32,33]

Column type	Particle-packed[b]	Porosity[a] Monolithic silica column		
		MS-PTFE(C)-S	MS-PEEK	MS-FS
Column diameter	4.6 mm	7 mm	4.6 mm	100 μm
Column length	15 cm	8.3 cm	10 cm	25 cm[c]
Total porosity	0.78	0.86	(0.87)	0.96
Through-pore[d]	0.39	0.62	(0.69)	0.86
Mesopore	0.40	0.24	(0.18)	0.10

[a] Porosity of monolithic silica column measured by size exclusion chromatography in THF using polystyrene standards and alkylbenzenes. The porosities in parentheses were obtained with C_{18}-bonded phase.
[b] Develosil-C_{18} particles packed in a column, 4.6 mm diameter, 10 cm in length.
[c] Effective length between the inlet and the detection window. Total length, 33.5 cm.
[d] External porosity.

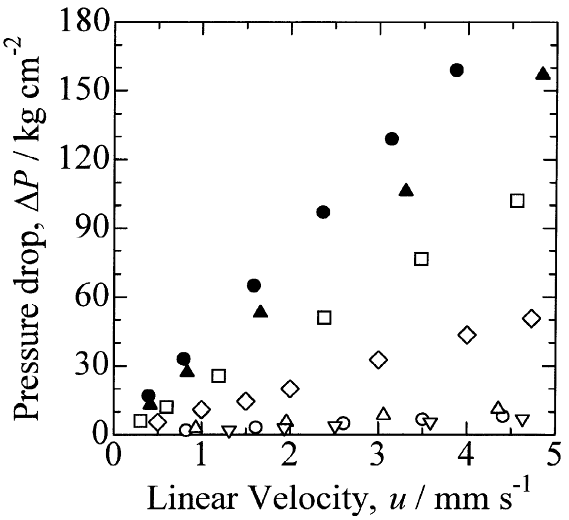

Fig. 4. Plots of column back pressure against linear velocity of mobile phase [29,32,37]. Mobile phase: 80% methanol. The pressures were normalized to the column length of 15 cm. Columns: 5 μm silica-C_{18} particles, Mightysil RP18 (●), Inertsil ODS-3 (▲). Monolithic silica column prepared in a mold, MS-PTFE(B)S-C_{18} (◇), MS-PEEK (□). Monolithic silica column in capillary, MS-FS(50)-A (○), MS-FS(50)-B (△), MS-FS(50)-C (▽). MS-FS(50); 50 μm I.D.× (A) 33.5 cm (effective length 25 cm), (B) 53.5 cm (effective length 45 cm), (C) 138.5 cm (effective length 130 cm).

provided by the presence of large through-pores and relatively small-sized skeletons resulted in the lower plate height and the lower pressure drop with monolithic silica columns compared with a particle-packed column, making faster separations possible with current instrumentation. Fig. 5a and b shows the chromatograms obtained with MS-PEEK and Inertsil ODS-3 for alkylbenzenes in 80% methanol–water. At low linear velocity of ca. 1 mm/s, the particle-packed column, Inertsil ODS-3 (15 cm) and MS-PEEK (10 cm) showed similar column efficiency, about 12 000 theoretical plates, but at higher linear velocity MS-PEEK column showed better performance than the particle-packed column.

Although it is hard to prepare a long MS column in a mold, a column of up to 150 cm can be prepared in a capillary. Such columns showed even higher permeability, allowing the generation of a large number of theoretical plates. Fig. 5c–e shows the chromatograms obtained with three monolithic silica columns (MS-FS(50)-A 25 cm; MS-FS(50)-B 45 cm, and MS-FS(50)-C 130 cm) for alkylbenzenes in 80% acetonitrile at a linear velocity of ca. 1 mm/s. Excellent peak symmetry was observed. At low linear velocity of 0.9 mm/s, MS-FS(50)-A produced 16 000 theoretical plates in 80% acetonitrile that are similar to the efficiency of a common 15-cm column packed with 5-μm particles, but at much lower pressure drop of 0.7 kg/cm^2. Fig. 5e shows that the 130-cm column (MS(50)-C) produced 106 000 theoretical plates for hexylbenzene at 0.9 mm/s linear velocity with pressure drop of 3.7 kg/m^2. At a higher linear velocity (4.7 mm/s), MS(50)-C produced 50 000–60 000 theoretical plates at 28 kg/cm^2 with t_0 of 4.5 min (Fig. 5f). Fig. 5f suggests that it is possible to generate 100 000 theoretical plates with t_0 of 9 min and at ca. 60 kg/cm^2 under similar conditions by using a 250-cm column. Such a column would generate nearly 200 000 theoretical plates at a lower linear velocity.

As is the case of particle-packed columns, higher column efficiency was obtained with a monolithic silica column with smaller domain size that results in higher pressure drop. The monolithic silica columns having domain size of 5.8, 3.8, 2.9, and 2.3 μm, showed the minimum plate height of 15, 7, 8, and 5 μm, respectively, for amylbenzene in 80% methanol [29].

Fig. 6a shows the van Deemter plots obtained with amylbenzene as a solute in 80% methanol by using columns of 4.6–7 mm diameter. MS-PEEK (Ref. [40], through-pore size = 2 μm) and MS-PTFE (SR-(B)-S-C_{18} of Ref. [29] through-pore size = 2.2 μm) showed lower plate height, especially at high linear velocities than a column packed with 5-μm particles. The small-sized silica skeletons, estimated to be 1.5 μm and 1.6 μm for MS-PEEK and MS-PTFE(B), respectively, resulted in small increase in plate height with the increase in linear velocity, as seen from the small slope of the van Deemter plot. It should be noted that these monolithic silica columns showed much lower pressure drop than the particle-packed columns, as shown in Fig. 4.

Fig. 6b indicates that the MS-FS(50) columns showed much lower column efficiency than a monolithic silica column prepared in a mold, in spite of the similar skeleton size (2 μm). Plate height minimum was not found for MS-FS(50) columns above linear velocity of 0.8 mm/s. The performance of

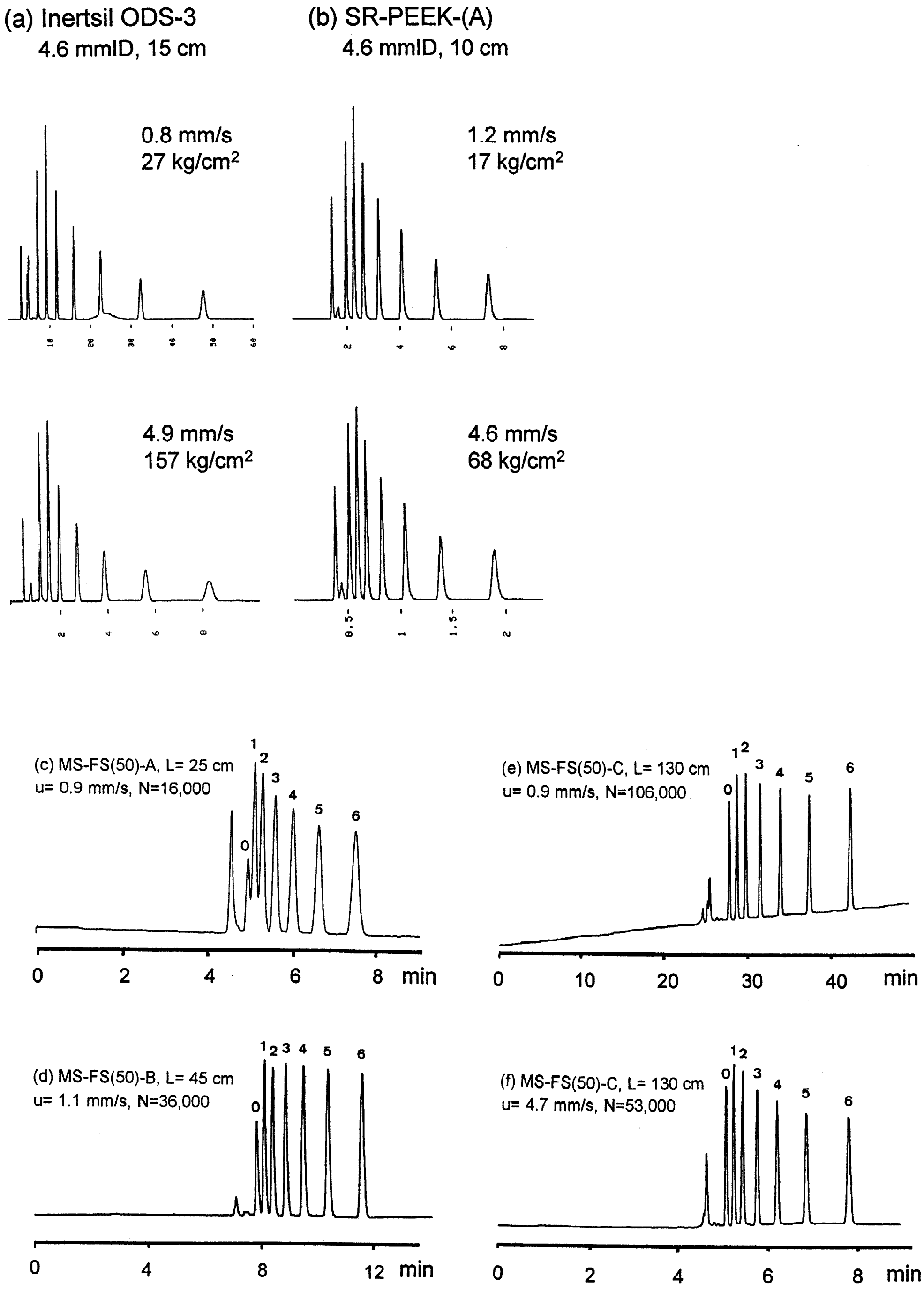

Fig. 5. Chromatograms obtained for alkylbenzenes ($C_6H_5C_nH_{2n+1}$, $n=0$–6) [32,37]. (a) Inertsil ODS-3 (5 μm particles), 4.6 mm I.D., 15 cm, (b) MS-PEEK column, 4.6 mm I.D., 10 cm. Mobile phase: 80% methanol. The linear velocity and the pressure drop are indicated. (c–f) Chromatograms obtained for alkylbenzenes ($C_6H_5C_nH_{2n+1}$, $n=0$–6) on MS-FS columns. (c) MS-FS(50)-A: column size: 50 μm I.D.×33.5 cm (effective length 25 cm), (d) MS-FS(50)-B: 50 μm I.D.×53.5 cm (effective length 45 cm), (e, f) MS-FS(50)-C: 50 μm I.D.×138.5 cm (effective length 130 cm). Mobile phase: 80% acetonitrile. The linear velocity and the pressure drop are indicated.

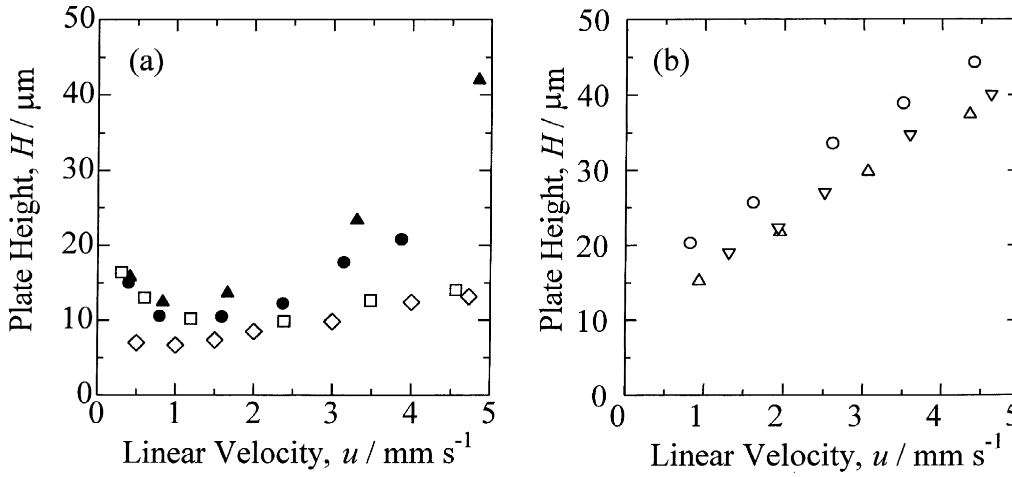

Fig. 6. The van Deemter plots obtained for C_{18} monolithic silica columns and silica-C_{18} packed column with hexylbenzene as a solute [29,32,37]. (a) For columns of 4.6–7 mm I.D., (b) for MS-FS(50) A, -B, and -C. Mobile phase: 80% methanol. Symbols as in Fig. 4 for the columns.

MS-FS(50) columns prepared in the presence of urea, however, was much better than that of a monolithic silica column prepared in the absence of urea in a capillary of 100 μm diameter [33,37]. The reproducibility of preparation in terms of plate height and pressure drop was within ±15% in most cases, while reproducibility was ca. ±5% for retention factors for individual preparations.

The MS-FS(50) column showed plate height of about 4 μm for hexylbenzene at 1 mm/s, and smaller plate height at higher linear velocities, when operated under CEC conditions in 80% acetonitrile–20% Tris-buffer. Therefore *B*-term contribution in 80% methanol that has higher viscosity than 80% acetonitrile is much smaller at $u = 1.5–5$ mm/s. *C*-term contribution to band broadening was also considered to be small for monolithic silica having 2-μm skeletons based on the results obtained with monolithic columns prepared in a mold having a similar skeleton size. Knox recently pointed out that the *A*-term (Eqs. (2) and (3)) makes a major contribution to band broadening on a particle-packed column in HPLC, while the *C*-term contribution is minor [41]:

$$H = A'u^m \tag{10}$$

$$H = 1/(1/A'_e + D_m/A'_m u) \tag{11}$$

With small *B*-term and *C*-term contribution for MS-FS(50) at a linear velocity range of 1.5–5 mm/s, one can characterize the dependence of H on u according to Eq. (10). Knox approximated the dependence by Eq. (10) with $m = 0.3–0.4$ in HPLC at very high linear velocities where the *B*-term contribution can be neglected [41]. The plots in Fig. 7a showed a fair fit to Eq. (10) at $m = 0.5–0.6$. The greater dependence of H on u for the MS-FS column suggests the greater contribution of mobile phase mass transfer (A_m term) to band-broadening relative to eddy diffusion (A_e term). When the plots in Fig. 7 were fitted with Eq. (11), a fair fit was observed with an A'_e value of 50–80 indicating that the eddy diffusion term is very large, and therefore the plate height is mainly controlled by the A'_m term. The results suggest the major contribution of A term to plate height, especially the A_m term corresponding to the contribution of slow mobile phase mass transfer. Large A'_e values suggest the irregularity of structure, or the presence of both large and small through-pores in a monolithic silica column, and/or the inefficient exchange of streampaths due to the characteristic structure of through-pores that are wide and relatively straight compared to interstitial voids of a particle-packed column. The dominating effect of slow mobile-phase mass transfer is well known in open-tube liquid chromatography [2], where plate

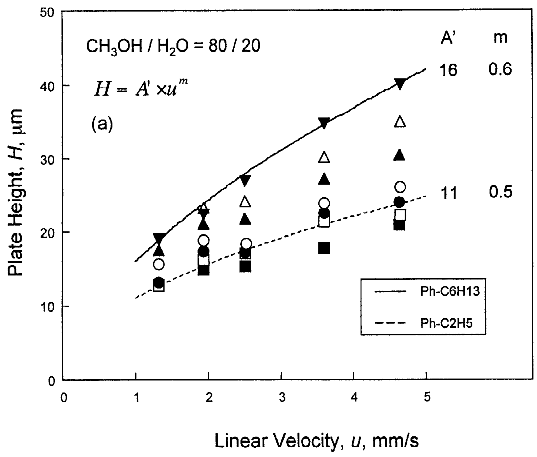

Fig. 7. (a) The simulation with Eq. (10) for the van Deemter plots in 80% methanol for ethylbenzene and hexylbenzene as solutes [37]. Column: MS-FS(50)-C. Mobile phase: 80% methanol. Samples: alkylbenzenes ($C_6H_5(CH_2)_nH$, $n=0$–6). $n=0$ (■), 1 (□), 2 (●), 3 (○), 4 (▲), 5 (△), 6 (▼). The curves were obtained with $n=0.50$ (ethylbenzene) and 0.60 (hexylbenzene) in Eq. (10), as shown in the figure. A' value (Eq. (10)) was adjusted to give the fit to the experimental points. (b) The simulation with Eq (11) for the van Deemter plots in 80% methanol for ethylbenzene and hexylbenzene as solutes. Column: MS-FS(50)-C. The curves were obtained with $A'_e=50$ (ethylbenzene) and 80 (hexylbenzene) in Eq. (11), as shown in the figure. The D_m values were calculated using the Wilkie–Chang equation [42]. A'_m value was adjusted to give the best fit to the experimental points.

height shows nearly linear dependence on the linear velocity and strong dependence on retention factors. The latter was also seen in Fig. 7. Because the performance of the present monolithic silica in capillary seems to be dominated by the A term in the velocity range studied, particularly large A_m caused by the presence of the large through-pores together with large A_e, much better performance can be expected in CEC, as observed [33], and for monolithic silica columns having smaller through-pore size. The preparation of a column of smaller A term (smaller through-pores) and the preparation with high reproducibility will be a subject of study for MS-FS columns.

The column efficiency of the MS-FS(50) per unit length was lower than that of a column packed with 5-μm particles by a factor of about two in a low velocity region (Fig. 6). The pressure drop of MS-FS(50), however, was about 1/25–1/30 that of such a conventional column (Fig. 4). Thus it was possible to generate more than 100 000 theoretical plates at very low pressure by using a long capillary column, as shown in Fig. 5e. It should be noted that reported column efficiencies in CEC are usually 50 000–100 000 theoretical plates per column of 20–30 cm [43].

High performance of an MS column is shown by the smaller separation impedance, E value, than that of a column packed with particles in Fig. 8. The minimum separation impedance, E value, of ca. 200–

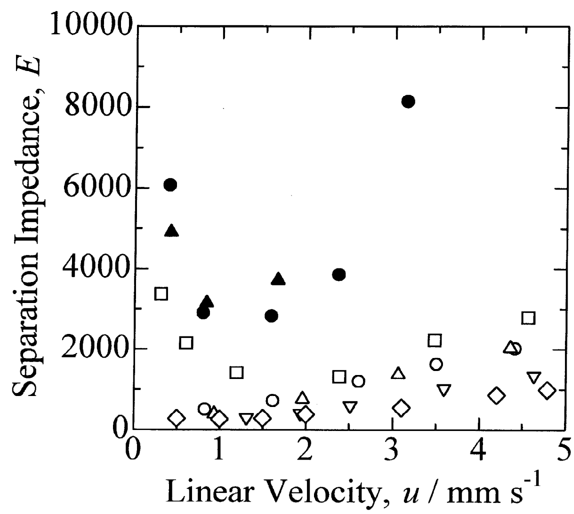

Fig. 8. Plots of separation impedance against linear velocity of mobile phase calculated for hexylbenzene as a solute [29,32,37]. Mobile phase: 80% methanol. Symbols as in Fig. 4 for the columns.

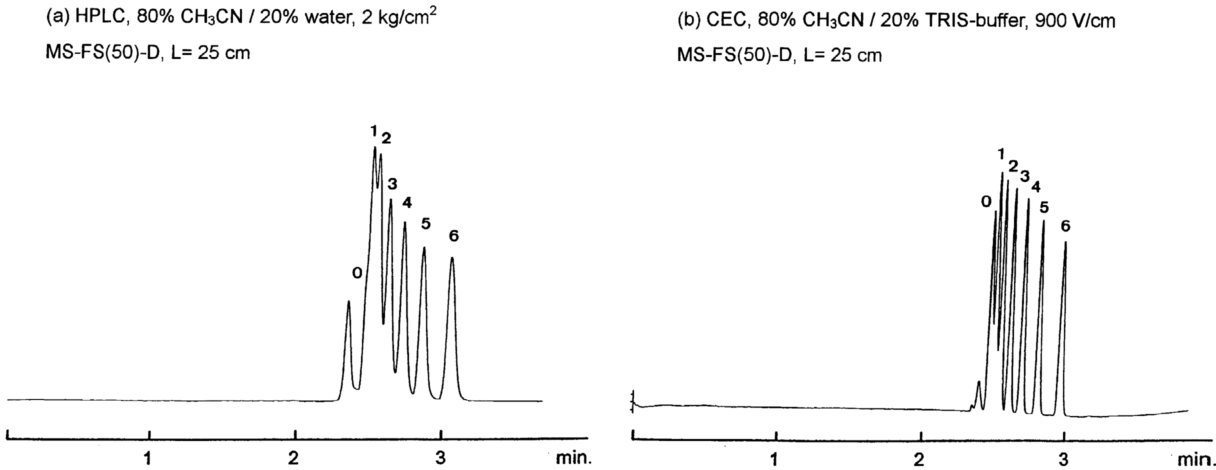

Fig. 10. Chromatograms obtained for alkylbenzenes ($C_6H_5C_nH_{2n+1}$, $n=0$–6) in pressure-driven (HPLC (a)) and electrodriven elution (CEC (b)). Column size: MS-FS(50)D, 50 μm I.D.×33.5 cm (effective length 25 cm). Mobile phase: (a) 80% acetonitrile, (b) acetonitrile–Tris–HCl 50 m*M* pH 8 (80/20). Pressure (a): 2 kg/cm^2. Applied voltage (b): 900 V/cm.

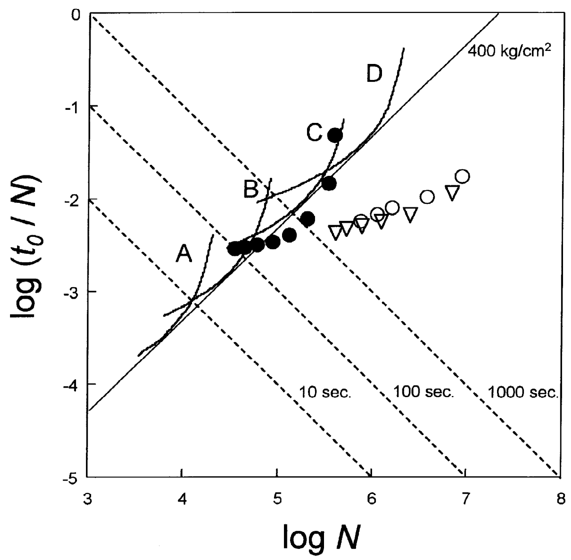

Fig. 11. Plots of plate time, (t_0/N), vs. plate number with particle-packed column and monolithic columns (adopted for 80% acetonitrile mobile phase from Ref. [2]) [37]. The curves for a column packed with particles were obtained by assuming the parameters, maximum pressure: 400 kg/cm^2, $\eta=0.00047$ Pa/s, $\phi=1000$, $D_m=2.1\times10^{-9}$ m^2/s, and Knox equation $h=\nu^{1/3}+1.5/\nu+0.05\nu$. Particle diameter: (A) 1 μm, (B) 2 μm, (C) 5 μm, (D) 10 μm. The points are based on the experimental results in 80% acetonitrile on a monolithic column, MS(50)-A (○), MS(50)-C (▽) and a particle-packed column, Mightysil RP18 (●), extrapolated to the limiting conditions of 400 kg/cm^2. The dashed lines indicate the required t_0 values in seconds.

umns for particle sizes of 1, 2, 5, and 10 μm, assuming 400 kg/cm^2 as the pressure limit. The plots for the 5-μm C_{18} particle-packed column, Mightysil RP18, and the C_{18} monolithic silica in capillary, MS-PEEK, MS-FS(50)-A and MS-FS(50)-C, are based on the experimental results, extrapolated to the limiting pressure of 400 kg/cm^2. A commercial column, Mightysil RP18, provided high efficiency close to the predicted performance for 5-μm particles.

The plots experimentally obtained for MS(50)-A and MS(50)-C clearly indicate the advantage of the monolithic structure for producing high column efficiency beyond the limit of performance of a column packed with particles under pressure-driven conditions. The plots in Fig. 11 suggest that a column of MS(50)-C type can potentially produce ~100 000 with 400 s t_0 at 100 kg/m^2. A particle-packed column would need 400 kg/m^2 to achieve such efficiency. The present study showed that one way to generate a large number of theoretical plates in HPLC is to use a long capillary-type monolithic silica column possessing high permeability. Although the use of such a column in HPLC will need longer separation time than CEC to achieve similar efficiency, the former will have less practical difficulty and is easy to hyphenate with an MS detector. Because the major source of band broadening is the slow mobile-phase mass transfer, monolithic silica columns with smaller domain size than the present columns should be developed to generate much higher column efficiency in high-speed separations [37], as experienced with the use of small particles in the course of the column development in HPLC.

5. Improvement in performance under CEC conditions

Since the major source of band broadening in pressure-driven operation of monolithic silica columns in a capillary is the slow mobile-phase mass transfer, CEC application is very attractive. Actually plate numbers in CEC were found to be greater than in HPLC by nearly 3–4 times for the same column [33], as shown in Fig. 10. However, an ODS phase having maximum surface coverage prepared by using octadecyldimethylchlorosilane resulted in slow separation and relatively low efficiency as a column having 2 μm silica skeletons due to the slow electroosmotic flow. Under most favorable conditions, MS-FS(50) column with low surface coverage with C_{18} groups showed plate height of ca. 3–4 μm producing up to 80 000 theoretical plates for 25-cm column length in 80% acetonitrile–20% aqueous buffer (pH 8) [45]. It was shown that faster and more efficient separation could be achieved (i) with an ODS phase with low surface coverage, (ii) with an ODS phase prepared by using octadecyltrichlorosilane, or (iii) by pressure-assisted CEC utilizing the high permeability of monolithic silica columns [45]. It would be desirable to prepare monolithic silica columns that can produce high electroosmotic flow without sacrificing the chemical and chromatographic properties of monolithic silica columns.

6. Future prospects

The characterization of monolithic silica columns indicates that MS-PTFE and MS-PEEK provide high performance based on the small skeleton size and the through-pore size that is slightly larger than the skeleton size, while MS-FS columns provide high performance based on the extremely large through-pores. The large (through-pore size/skeleton size) ratios obtainable with a monolithic column resulted in higher performance with simple pressure-driven elution utilizing current instrumentation. MS-PEEK will be useful for faster separations, and long MS-FS columns for high efficiency separations. Monolithic silica columns were also shown to be effective for the separation of high-molecular-weight solutes.

The disadvantages associated with monolithic silica columns include the following.

(i) Individual monolithic columns must be prepared and chemically modified one at a time.
(ii) When they are prepared in a mold, the bare silica rod must be covered by column materials, such as PEEK.
(iii) Individual preparation and subsequent chemical bonding can lead to problems in reproducibility.
(iv) Chemical modification must be carried out on-column.

Nevertheless, the possibility of providing ultrahigh performance with current instrumentation that is not possible with a column packed with particles, and the compatibility of monolithic columns with other techniques including CEC and UHPLC as well as the applicability for chip chromatography [44] will make monolithic columns an attractive separation medium in the future. Future work should include the reduction of domain size and the increase in reproducibility of preparation [37]. The development of the preparation method of a capillary column of a wider size range or in channels on a chip will also be of practical importance.

Acknowledgements

The authors wish to thank Dr. Lloyd R. Snyder for his helpful suggestions on the characterization of the monolithic silica columns. The research on monolithic silica columns was supported in part by a Grant-in-Aid for Scientific Research funded by the Ministry of Education, Sports, Culture, Science, and Technology. The support by Merck is also gratefully acknowledged.

References

[1] J.C. Giddings, Dynamics of Chromatography, Part 1, Principles and Theory, Marcel Dekker, New York, 1965.

[2] H. Poppe, J. Chromatogr. A 778 (1997) 3.
[3] P.A. Bristow, J.H. Knox, Chromatographia 10 (1977) 279.
[4] J.E. MacNair, K.C. Lewis, J.W. Jorgenson, Anal. Chem. 69 (1997) 983.
[5] J.E. MacNair, K.D. Patel, J.W. Jorgenson, Anal. Chem. 71 (1999) 700.
[6] M.M. Dittmann, G.P. Rozing, J. Chromatogr. A 744 (1996) 63.
[7] F.D. Antia, Cs. Horváth, J. Chromatogr. 435 (1988) 1.
[8] K.K. Unger, Porous Silica, Elsevier, Amsterdam, 1979, Chapter 5.
[9] F. Svec, J.M.J. Frechet, Anal. Chem. 64 (1992) 820.
[10] Q.C. Wang, F. Svec, J.M.J. Frechet, Anal. Chem. 65 (1993) 2243.
[11] C. Fujimoto, J. Kino, H. Sawada, J. Chromatogr. A 716 (1995) 107.
[12] C. Ericson, J.-L. Liao, K. Nakazato, S. Hjerten, J. Chromatogr. A 767 (1997) 33.
[13] E.C. Peters, M. Petro, F. Svec, J.M.J. Frechet, Anal. Chem. 70 (1998) 2296.
[14] E.C. Peters, F. Svec, J.M.J. Frechet, Adv. Mater. 11 (1999) 1169.
[15] I. Gusev, X. Huang, C. Horvath, J. Chromatogr. A 855 (1999) 273.
[16] A. Palm, M.V. Novotny, Anal. Chem. 69 (1997) 4499.
[17] A. Maruska, C. Ericson, A. Vegvari, S. Hjerten, J. Chromatogr. A 837 (1999) 25.
[18] F. Svec, E.C. Peters, D. Sykora, C. Yu, J.M.J. Frechet, J. High Resolut. Chromatogr. 23 (2000) 3.
[19] M.T. Dulay, R.P. Kulkarni, R.N. Zare, Anal. Chem. 70 (1998) 5103.
[20] C.K. Ratnayake, C.S. Oh, M.P. Henry, J. High Resolut. Chromatgr. 23 (2000) 81.
[21] R. Asiaie, X. Huang, D. Farnan, C. Horvath, J. Chromatogr. A 806 (1998) 251.
[22] Q. Tang, M.L. Lee, J. High Resolut. Chromatogr. 23 (2000) 73.
[23] T. Adam, K.K. Unger, M.M. Dittmann, G.P. Rozing, J. Chromatogr. A 887 (2000) 327.
[24] K. Nakanishi, J. Porous Mater. 4 (1997) 67.
[25] K. Nakanishi, H. Shikata, N. Ishizuka, N. Koheiya, N. Soga, J. High Resolut. Chromatogr. 23 (2000) 106.
[26] N. Tanaka, H. Kobayashi, K. Nakanishi, H. Minakuchi, N. Ishizuka, Anal. Chem. 73 (2001) 420A.
[27] H. Minakuchi, K. Nakanishi, N. Soga, N. Ishizuka, N. Tanaka, Anal. Chem. 68 (1996) 3498.
[28] H. Minakuchi, K. Nakanishi, N. Soga, N. Ishizuka, N. Tanaka, J. Chromatogr. A 762 (1997) 135.
[29] H. Minakuchi, K. Nakanishi, N. Soga, N. Ishizuka, N. Tanaka, J. Chromatogr. A 797 (1998) 121.
[30] H. Minakuchi, N. Ishizuka, K. Nakanishi, N. Soga, N. Tanaka, J. Chromatogr. A 828 (1998) 83.
[31] K. Cabrera, G. Wieland, D. Lubda, K. Nakanishi, N. Soga, H. Minakuchi, K.K. Unger, Trends Anal. Chem. 17 (1998) 50.
[32] N. Tanaka, H. Nagayama, H. Kobayashi, T. Ikegumi, K. Hosoya, N. Ishizuka, H. Minakuchi, K. Nakanishi, K. Cabrera, D. Lubda, J. High Resolut. Chromatogr. 23 (2000) 111.
[33] N. Ishizuka, H. Minakuchi, K. Nakanishi, N. Soga, H. Nagayama, K. Hosoya, N. Tanaka, Anal. Chem. 72 (2000) 1275.
[34] M.S. Fields, Anal. Chem. 68 (1996) 2709.
[35] C. Fujimoto, J. High Resolut. Chromatogr. 23 (2000) 89.
[36] J.D. Hayes, A. Malik, Anal. Chem. 72 (2000) 4090.
[37] N. Ishizuka, H. Kobayashi, H. Minakuchi, K. Nakanishi, K. Hirao, K. Hosoya, T. Ikegami, N. Tanaka, J. Chromatogr. A, in press.
[38] A.P. Karnaukhov, in: S. Modry (Ed.), Proceedings of Rilem/IUPAC International Symposium on Pore Structure and Properties of Materials, Vol. I, Academia, Prague, 1974, p. A3.
[39] T. Hashimoto, M. Itakura, H. Hasegawa, J. Chem. Phys. 85 (1986) 6118;
T. Hashimoto, M. Itakura, H. Hasegawa, J. Chem. Phys. 85 (1986) 6773.
[40] K. Cabrera, D. Lubda, H.-M. Eggenweiler, H. Minakuchi, K. Nakanishi, J. High Resolut. Chromatogr. 23 (2000) 93.
[41] J.H. Knox, J. Chromatogr. A 831 (1999) 3.
[42] C.R. Wilkie, P. Chang, Am. Inst. Chem. Eng. J. 1 (1955) 264.
[43] K.D. Bartle, P. Myers, J. Chromatogr. A 916 (2001) 3.
[44] C. Ericson, J. Holm, T. Ericson, S. Hjerten, Anal. Chem. 72 (2000) 81.
[45] H. Kobayashi, C. Smith, K. Hosoya, T. Ikegami, N. Tanaka, Anal. Sci. 18 (2002) 89.